2006

Electrochemic properties of single-wall carbon nanotube electrodes

J. N. Barisci
University of Wollongong

G G. Wallace
University of Wollongong, gwallace@uow.edu.au

D. Chattopadhyay
University of Conneticut, USA

F. Papadimitrakopoulos
University of Conneticut, USA

R. H. Baughman
University of Texas, USA

Journal of The Electrochemical Society, **150** (9) E409-E415 (2003)
0013-4651/2003/150(9)/E409/7/$7.00 © The Electrochemical Society, Inc.

Electrochemical Properties of Single-Wall Carbon Nanotube Electrodes

Joseph N. Barisci,[a,*,z] Gordon G. Wallace,[a] Debjit Chattopadhyay,[b] Fotios Papadimitrakopoulos,[b] and Ray H. Baughman[c]

[a]*Department of Chemistry, University of Wollongong, New South Wales 2522, Australia*
[b]*Department of Chemistry, University of Connecticut, Storrs, Connecticut 06269, USA*
[c]*Nano Tech Institute, The University of Texas at Dallas, Richardson, Texas 75083-0688, USA*

The electrochemical properties of single-wall carbon nanotube (CNT) electrodes in the form of sheets or papers have been examined. Thermal annealing has produced significant changes in a range of properties of the material including increased hydrophobicity and elimination of electroactive surface functional groups and other impurities. As a result of these changes, the treated electrodes exhibit lower double-layer capacitance, absence of faradaic responses and associated pseudocapacitance, and a better frequency response. The basic electrochemical behavior of the CNT paper electrodes is not markedly affected by relatively large differences in electrolyte ion size, consistent with an average pore size of 9 nm. Increases in both CNT sheet thickness and surface area induce a slower electrode response in agreement with the porous nature of the electrode matrix.
 [DOI: 10.1149/1.1593045]

Manuscript submitted September 25, 2002; revised manuscript received March 5, 2003. Available electronically July 10, 2003.

The exciting scientific and technological possibilities offered by carbon nanotubes (CNTs) are the focus of significant research efforts. The growing literature on the subject, summarized and reviewed in recent publications,[1-5] is now providing new insights into the fundamental properties of CNTs while pointing to some practical applications. Many of these applications are electrochemical in nature because CNTs possess many of the properties that have made carbon electrodes so useful in the past. However, the special structure of CNTs suggests that other, new interesting properties are likely to be of use to scientists and technologists in general, not just to electrochemists.

The electrochemical applications of CNT include capacitors,[6,7] batteries,[8,9] and electromechanical actuators.[10,11] Our interest stems from the ability of single-wall CNTs to undergo dimensional changes (expand and contract) upon the application of appropriate potentials. Using a suitable device configuration, these volume changes can be used to do mechanical work. Electromechanical actuation by CNT electrodes, fabricated in a form described as mats, sheets, or papers, has been demonstrated in primitive devices.[10,11] However, improvements are needed if practical devices are to be made possible. The areas to be improved are many, but, from the electrochemical point of view, some parameters are clearly more important, and they are the subject of our attention.

Initial work on electromechanical actuators used untreated CNT paper electrodes.[12] Because this unannealed nanotube paper contains redox active impurities (resulting from acid treatments used to remove forms of carbon other than the nanotubes), we now typically thermally anneal acid-treated nanotube paper before use in actuators. In previous reports,[13-15] we described some of the fundamental electrochemical properties of mainly unannealed single-wall CNT electrodes. Here, we report new studies that focus on annealed CNT paper and its characterization, which in this case has included electrochemical impedance spectroscopy (EIS). As in previous work, factors particularly important for electromechanical actuators have received special attention. They include capacitance and the ability to store charge, charging rate and frequency response, effect of thermal treatment, effect of electrode thickness and surface area, and effect of electrolyte nature and concentration.

Experimental

Chemicals and materials.—All aqueous solutions were prepared using Milli-Q deionized water. Single-wall CNTs dispersed in water or toluene were obtained from Tubes@Rice (Rice University Houston, Texas). The material consists of hexagonally packed bundles of nanotubes 1.2-1.4 nm diam. Each bundle consists of about 30-100 nanotubes, with average diam 50-140 nm and lengths in the micrometer scale.[16]

Instrumentation.—A conventional three-electrode cell was used for all electrochemical experiments. The working electrode was a piece (~0.3 cm^2) of CNT paper attached to a short piece of thin platinum wire, the reference electrode was Ag/AgCl (3 M NaCl) for aqueous media and Ag/Ag^+ (0.01 M $AgClO_4$/0.1 M tetrabutylammonium perchlorate/acetonitrile) for nonaqueous solutions, and the auxiliary electrode consisted of a piece of CNT paper several times larger than the working electrode. The potentiostat for cyclic voltammetry (CV) and chronoamperometry consisted of PAR 174/175 modules. A MacLab 4e (ADInstruments) interface operated by Chart software (ADInstruments) and a Macintosh computer were used to drive the potentiostat and to record its output. Electrochemical impedance data were obtained with an EG&G basic electrochemical system potentiostat operated by PowerSuite software (EG&G) and an Optima computer. Equivalent electrical circuit analysis was performed with EQUIVCRT.PAS software by B. Boukamp based on a nonlinear least-squares fit program and supplied by EG&G.

The surface area of the CNT papers was measured by the standard Brunauer, Emmett and Teller method (BET) using a Quanta Chrome NOVA 1000 adsorption isotherm machine. The technique involves adsorption of nitrogen gas by the substrate which is maintained at liquid nitrogen temperature. Before starting the actual physisorption, all the samples were degassed under vacuum at 200°C for 2 h to eliminate most of the physisorbed gases.

Porosimetry analysis was performed in a TriStar 3000 analyzer (Micromeritics) using nitrogen at 77 K. The pore size distribution was extracted from adsorption isotherms.

Contact angle measurements were performed using a Rame-Hart Goniometer (model 100-00-115) equipped with an environmental chamber. Typically, a drop of deionized water or aqueous electrolyte was placed on the surface of the CNT sample to determine the wetting characteristics.

Procedures.—The fabrication of the CNT paper has been previously described.[10,16] It involved vacuum filtration of the single-wall CNT suspension on a membrane filter, washing with water and methanol, air drying, and removal of the formed film from the filter. The CNT papers were subsequently vacuum dried at 80-120°C for 24 h.

All CNT paper electrodes were cycled in the electrolyte between ±0.8 V *vs.* Ag/AgCl or ±1.0 V *vs.* Ag/Ag^+ for five cycles at 50 mV/s before any measurements were made. Solutions were not deoxygenated unless otherwise indicated.

* Electrochemical Society Active Member.
z E-mail: nbarisci@uow.edu.au

Table I. Physical and electrochemical data for CNT papers.

Sample	Thickness (A)[a] (μm)	Density (A)[a] (g/cm^3)	Capacitance[b] (U)[a] (F/g)	Capacitance[b] (A)[a] (F/g)	R_1C[c] (A)[a] (ms)
Thin	22.5	0.30	30.4	12.7	23
Medium	29.0	0.35	29.5	13.8	26
Thick	36.5	0.41	35.9	13.9	35

[a] A: annealed, U: unannealed.
[b] Capacitance at 0.0 V in 1 M NaCl measured using CV.
[c] Time constant at 0.0 V in 1 M NaCl measured using chronoamperometry.

Annealing of the CNT paper was carried out under argon gas using the following temperature program: 20-120°C at 20°C/min, 120°C for 2 h, 120-300°C at 1°C/min, 300°C for 2 h, 300-600°C at 5°C/min, 600-1050°C at 10°C/min, 1050°C for 1 h, cool to room temperature overnight.

Results and Discussion

Effect of annealing.—Thermal treatment of the CNT paper in inert atmosphere produced a significant loss of mass (Table I), around 40%, in conjunction with a 26% decrease in sheet thickness, resulting in a lower density material. The bulk of the mass change is attributed to the volatilization of impurities resulting from acid-based removal of carbon contaminants, as well as from the surfactant added to disperse the CNT. However, the loss of some CNT is also probable.[4,5] Unless otherwise indicated, the results presented refer to annealed CNT samples.

CV.—As described previously,[13,15] annealing removed the broad redox responses observed in cyclic voltammograms of CNT paper in aqueous solutions. Capacitance measurements carried out on this occasion on the same samples, before and after annealing, revealed that the unannealed sample had values 2-3 times larger (Table I).

Two major factors may explain the observed differences. The first is related to the functional groups, such as carboxylic acid and quinone, which are attached to the surface of the CNT paper and give rise to a pseudocapacitance.[13,15] Elimination of these groups by heat-treatment removes this faradaic contribution.

A second factor, related to the annealing, is the increase in hydrophobicity of the CNT paper after treatment. The contact angle measured for unannealed CNT paper in 1 M NaCl solution was around 75°; whereas, upon annealing it was between 90-100°. The greater hydrophobicity results in decreased wetting of the CNT paper and hampers electrolyte penetration into the pores, thus lowering the capacitance.

Finally, in the unannealed samples, the CNTs are open and loosely packed, while it is known[16,17] that annealing increases crystallinity, allows the CNTs in the bundles to pack better, heals defects and closes the tubes ends, which were opened during the oxidative purification of the CNT, all of which could hinder wetting of the bundles.

EIS.—The complex plane impedance plots of annealed CNT paper electrodes have the general features expected for a porous electrode.[18,19] Two distinct domains are observed, a high-medium frequency domain with a characteristic linear portion approaching a 45° angle, and a low frequency region represented by an almost vertical straight line where the penetration depth of the ac signal approaches the pore depth and the electrode starts to behave like a flat surface (Fig. 1a). At the inflection point exhibited by the Nyquist plot, the frequency is about 250 Hz. At frequencies above 100 Hz, the impedance becomes increasingly resistive, while the value of the capacitance drops to a small fraction of its low frequency level, as shown later.

To further understand the basic electrochemical behavior of the CNT electrodes, some limited modeling was attempted. For the annealed electrode, the electrical equivalent circuit of Fig. 2a was used. This is a classical circuit where the double-layer capacitance has been replaced by a constant-phase element (CPE) that describes the frequency dispersion of the response. The CPE consists of a transmission line and an impedance given by $Z = [Q(j\omega)^n]^{-1}$, where $j = \sqrt{-1}$, Q is a constant combining the resistance and capacitance properties of the electrode, and n takes values between 0 and 1. Variations of the equivalent circuit of Fig. 2a were tested, but the best agreement with the experimental data was only observed when the proposed model was applied (Fig. 3a). Even here curve fitting in the high frequency region was not optimum, but the exercise still provided an indication of the basic electrode behavior. The value of n was in most cases around 0.95, indicating that the CPE_1 is essentially capacitive, considering that $n = 1$ for an ideal capacitor.

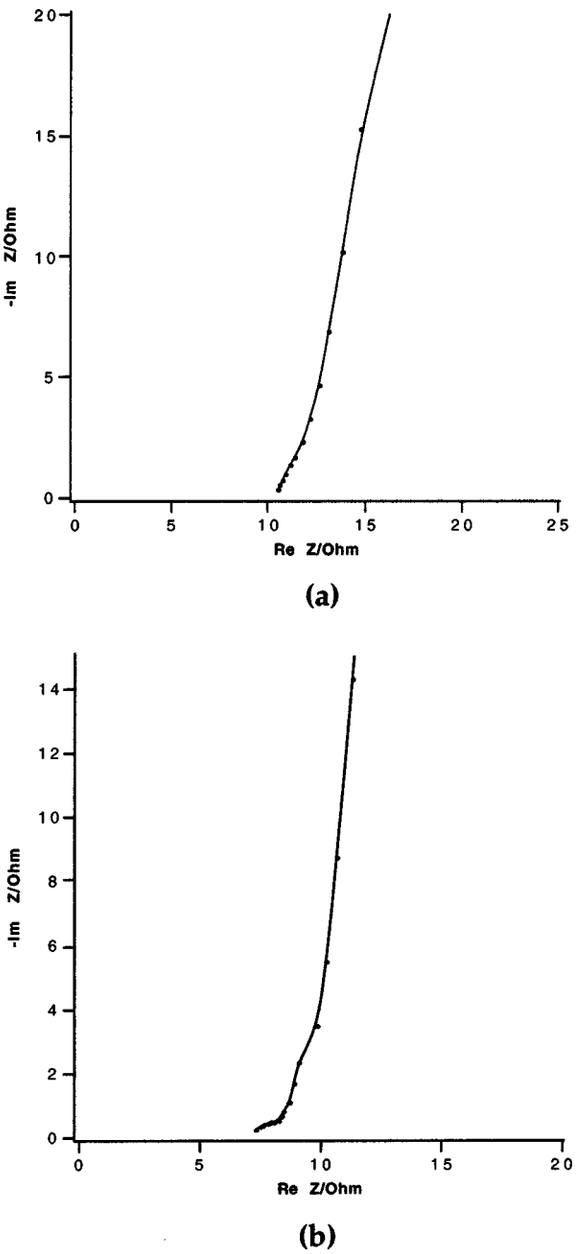

Figure 1. Nyquist plots for (a) annealed and (b) unannealed CNT paper electrodes at 0.0 V in 1 M NaCl.

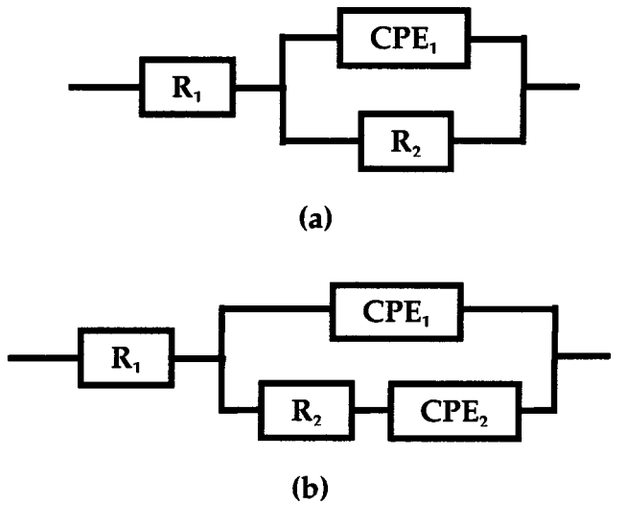

Figure 2. Equivalent circuits for (a) annealed and (b) unannealed CNT paper electrodes. R_1: resistance composed of solution resistance (R_s) and electrode resistance (R_e), R_2: charge-transfer resistance across electrode/solution interface, CPE_1: constant-phase element representing interfacial capacitance, CPE_2: constant-phase element representing pseudocapacitance from surface functional groups.

The capacitance values for the annealed CNT paper obtained from the impedance data correlated well with those obtained from CV, although the latter were slightly higher by around 10%. This is consistent with slow current components accessible by CV. In a porous electrode, the measured capacitance always has some scan rate or frequency dependence, which can be very strong in the case of diffusion/migration, concentration gradients, or charging of deep pores.

Consistent with the porous nature of the electrode, a capacitance dispersion is observed (Fig. 4), which is much stronger than that observed for the smoother basal plane of graphite.[20] When the frequency decreases, the capacitance tends to increase but reaches an almost constant value at low frequencies, below 5-10 Hz, depending on the sample. Above this frequency range, only part of the total length of the pores charges, and, as a consequence, the capacitance appears lower than the low frequency capacitance.

Unannealed CNT electrodes.—When the previous results are compared with those for the unannealed material, some differences are apparent. The Nyquist plot for the unannealed CNT paper (Fig. 1b) suggests the presence of an underlying semicircle in the high-medium frequency region, which can be explained by the pseudocapacitance associated with the surface-bound functional groups responsible for the responses observed in the cyclic voltammograms. Because of this additional feature, the equivalent circuit needed to fit the experimental results had to include an additional capacitive element in the form of a CPE representing the described pseudocapacitance (Fig. 2b and 3b).

The different natures of the annealed and unannealed materials were also evident, first, in the Bode phase-angle plot (not shown) where the maximum phase angle for the unannealed electrode appeared at lower frequencies, and second, in a stronger frequency dependence of the capacitance (Fig. 4). These results can be explained by the pseudocapacitance and by the greater penetration of the signal, due to the better wettability, exhibited by the unannealed electrode. The combination of these factors leads to a stronger frequency dependence of the signal for the unannealed CNT paper.

Effect of applied potential.—Potential of zero charge (pzc).—Determination of the pzc is important for carbon-based electromechanical actuators as its value indicates the potential at which the electrode volume would be minimum if dimensional changes

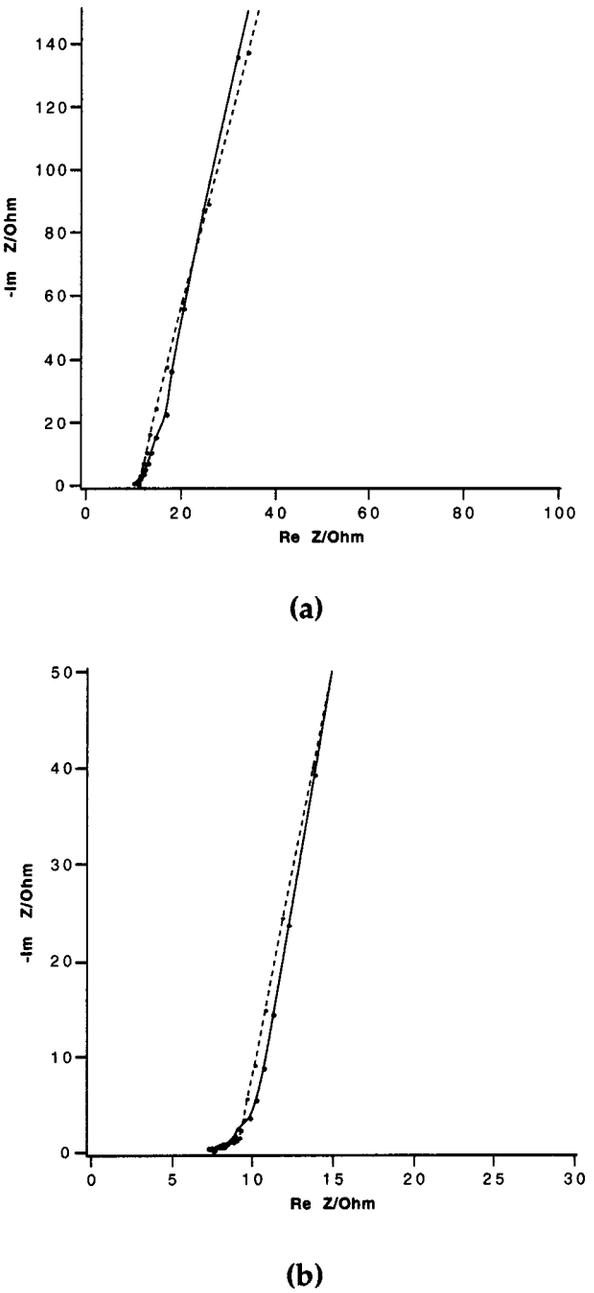

Figure 3. Nyquist plots for (a) annealed and (b) unannealed CNT paper electrodes at 0.0 V in 1 M NaCl showing experimental data (solid line) and simulated curves (dotted line) obtained from the equivalent circuits (Fig. 2).

were entirely electrostatic in origin.[21,22] Measurements of pzc were carried out in both aqueous and nonaqueous deoxygenated solutions by locating the potential at which the capacitance was minimum. In aqueous solution (0.005 M sodium chloride) the pzc was around 0.0 V (*vs.* Ag/AgCl), whereas in acetonitrile medium (0.005 M tetrabutylammonium hexafluorophosphate, TBAHFP) the pzc was around 0.0 V (*vs.* Ag/Ag^+). These values are very close to those reported for the basal plane of graphite,[20,23] particularly for nonaqueous solutions. The possible presence of residual surface oxide groups may be responsible for the slightly more positive value (by 0.15 V) obtained in aqueous solutions with respect to that observed for graphite. However, the pzc for the unannealed material in

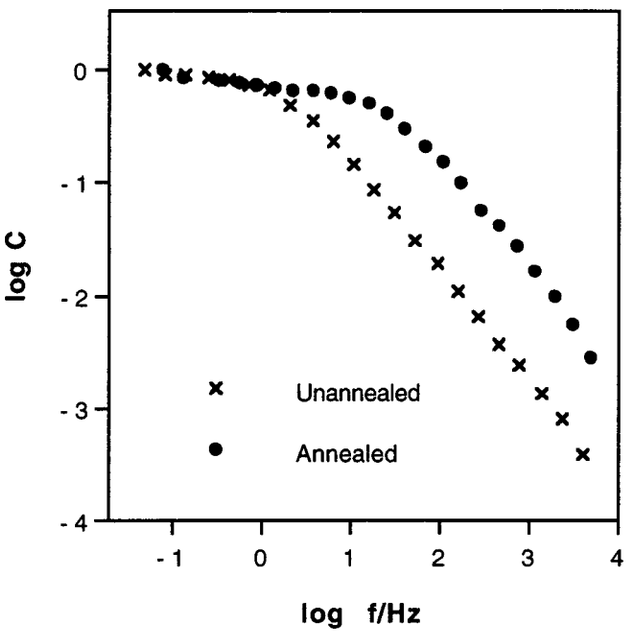

Figure 4. Capacitance as function of frequency for CNT paper electrodes, measured by EIS at 0.0 V in 1 M NaCl. Capacitance was normalized with respect to the maximum capacitance value.

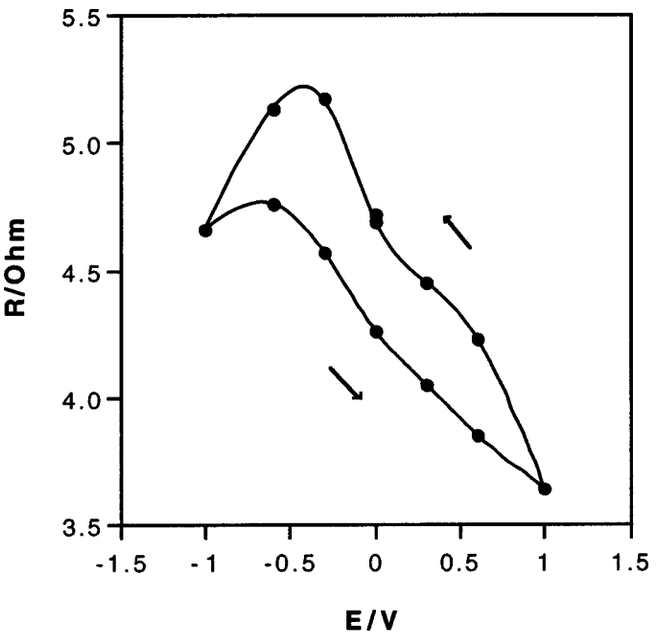

Figure 6. Resistance (R_1) as a function of applied potential for an annealed CNT paper electrode, measured by EIS in 1 M NaCl.

sodium chloride solution was up to 0.4 V more anodic, most likely due to the large presence of the surface oxygen-containing functional groups.

Capacitance.—Variation of the CNT paper capacitance over a wide range of applied potentials (±2 V) was investigated in 0.1 M TBAHFP in acetonitrile using EIS. The curve obtained has a parabolic shape with its minimum in the vicinity of the pzc (Fig. 5) and is similar to that reported for graphite,[20,23] albeit with a broader minimum. The same type of curve was obtained in aqueous solutions where a narrower potential range was used to avoid background solution reactions. As proposed for graphite,[20,23] the minimum in the capacitance-potential curve at high electrolyte concentrations is possibly due to the presence of a space-charge region within the CNT electrode, suggesting a material with semiconducting properties. The usual CNT material consists of a mixture of metallic and semiconducting CNTs.[4,5] As a result of a low density of electronic states near the Fermi level, a space-charge region exists in the solid. The absence of a sharp minimum in the capacitance-potential curve may be at least partly accounted by the surface heterogeneity of the porous CNT sheet. However, other factors such as the different nature of the space-charge layer in graphite and CNT may also play a role.

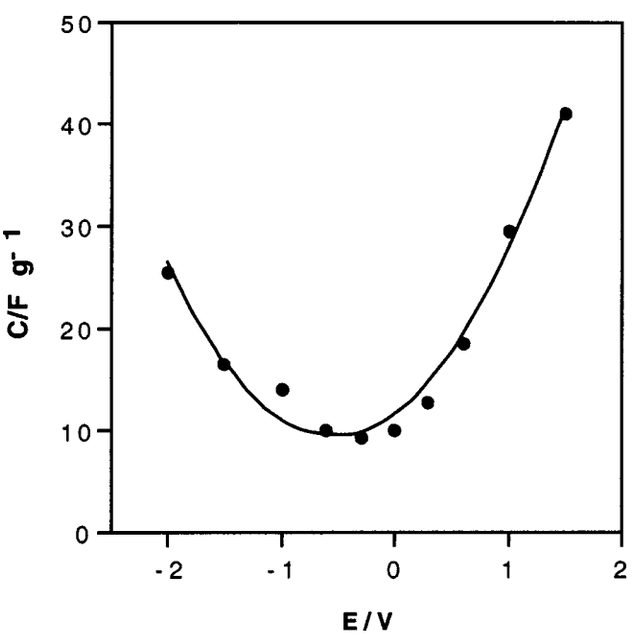

Figure 5. Capacitance as a function of applied potential for an annealed CNT paper electrode, measured by EIS in 0.1 M TBAHFP/acetonitrile.

Resistance.—Changing the applied potential produces a change, about 40% in the range −0.5 to 1.0 V, in the measured high frequency resistance (R_1), which is considered to include an electrode resistance (R_e) component (Fig. 2). The curve relating R_1 and the applied potential shows a maximum near the pzc (Fig. 6). This behavior is observed in both aqueous and nonaqueous solutions, and it always exhibits a clear hysteresis. A dependence of resistance on potential has been observed for graphite and other carbon materials,[24-26] and a possible explanation for this phenomenon has been suggested.[24,25]

The proposed model considers the carbon material as a semiconductor with a narrow bandgap and assumes a potential-dependent electronic conductivity, which is related to the population of both positive and negative charge carriers. At the potential of minimum conductivity, both types of carriers are present at their minimum concentrations. In addition, recent spectroscopic studies[27] on single-wall CNTs have shown that it is possible to electrochemically tune the electronic properties of the CNT, as a result of which maximum electronic resistance is observed around −0.3 V (*vs.* Ag/Ag^+), in agreement with our results. The suggested origin for these observations is the change in the number of free carriers resulting from electron depletion or filling of specific energy bands of the CNT as the Fermi level is shifted. It is also suggested that, associated with the electronic charging-discharging of the electrode, there is intercalation of electrolyte ions in the CNT films that act as dopants. This interpretation may explain the hysteresis observed in the resistance

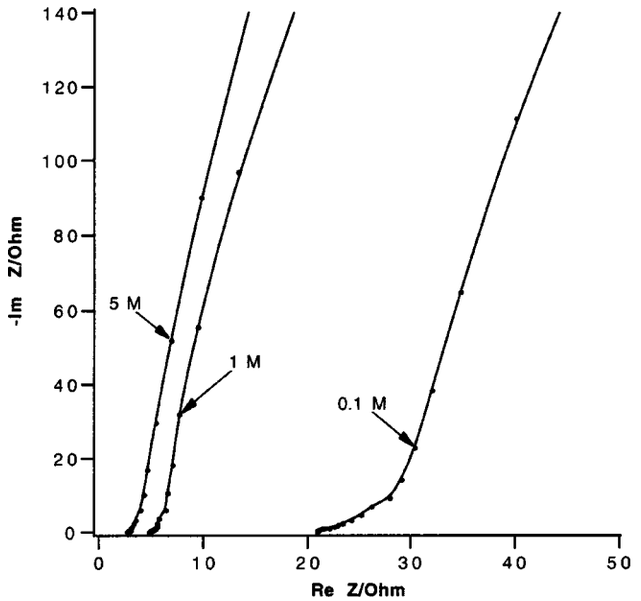

Figure 7. Nyquist plots for an annealed CNT paper electrode, obtained at 0.0 V in NaCl solutions of different concentrations.

change, as the intercalation processes probably only reach completion on a relatively slow time scale.[14]

As a result of the effect of applied potential on electrode resistance and capacitance, the time constant (R_1C) for electrode charging is also dependent on the potential. Although the potential has opposite effects on the variation of R_1 and C, the effect on C is stronger. Consequently, the time constant goes through a minimum (*e.g.*, ~100 ms in 0.1 M TBAHFP/acetonitrile) around the pzc and reaches values up to three times larger at applied potentials of ±1.5 V *vs.* pzc. This would have implications where fast charging and strain rates are important.

Effect of electrolyte nature and concentration.—Electrolyte concentration.—The influence of electrolyte concentration on the CNT paper electrochemical behavior was investigated using NaCl solutions with concentrations between 0.01 and 5.0 M. The capacitance increased by 60% and the resistance decreased about 60 times with increasing concentration within the range investigated. This resulted in an exponential decrease of the time constant (R_1C).

Impedance data showed that the frequency response depends greatly on the electrolyte concentration through the corresponding solution resistivities and by the need for the signal to penetrate into the electrode subsurface pores.

The plots in Fig. 7 illustrate how the ac response at the porous electrode becomes attenuated with increasing dilution of the invading electrolyte. The decrease in the slope and increase in the length of the 45° region of the Nyquist plot associated with decreasing electrolyte concentration are consistent with an increase in electrode pore resistance.[28,29] In dilute electrolyte solutions, the pore resistance becomes more significant and modifies the electrode response. Only at 1 M NaCl does the impedance response closely approach the expected behavior. In agreement with these effects, the capacitance dispersion is greater at the lower electrolyte concentrations.

Electrolyte type.—The influence of electrolyte anion on the electrochemical properties of the CNT paper was studied using aqueous solutions of Na^+ salts. These salts were selected to provide anions with diverse chemical properties, sizes, and electrical charges. The electrolyte solutions investigated contained 0.1 M Cl^-, 0.1 M NO_3^-, 0.1 M SO_4^{2-}, 0.1 M *p*-toluene sulfonate (PTS), 0.1 mM polystyrene sulfonate (PSS), and 4% w/v dextran sulfonate (Dex).

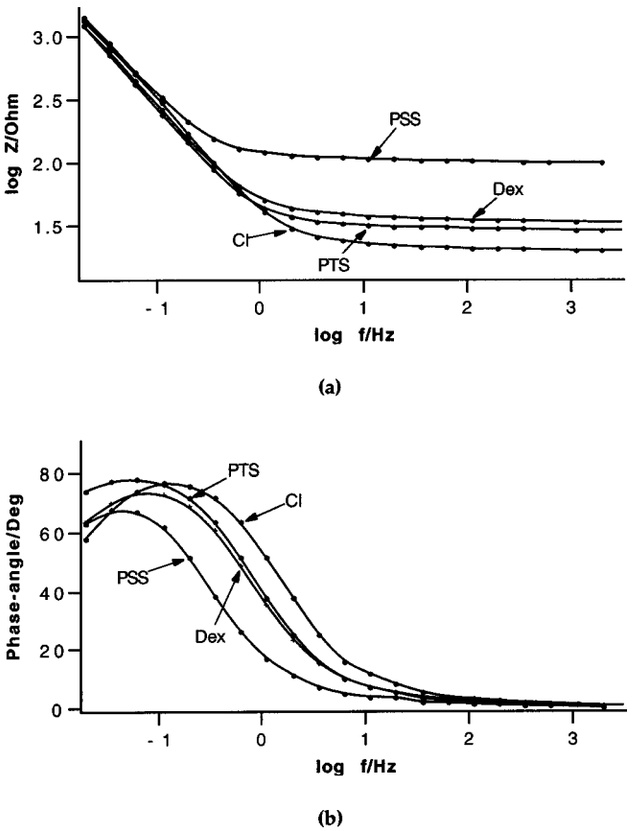

Figure 8. (a) Bode amplitude and (b) Bode phase-angle plots for an annealed CNT paper electrode, obtained at 0.0 V in different electrolyte solutions.

As was the case for unannealed CNT electrodes examined in electrolytes containing different anions and cations,[13-15] the cyclic voltammograms obtained for annealed electrodes were similar in all electrolyte solutions. The difference observed in the capacitance values for the smaller anions (Cl^-,NO_3^-,SO_4^{2-}) was not significant. For the other ions, the maximum difference was a 25% higher capacitance for PTS in relation to Cl^-, possibly due to some specific adsorption.[30] Impedance data (Fig. 8) indicated that within a relatively narrow range, the response of the CNT paper in PSS departed most from the average behavior, probably due to the increased resistance of this solution, 3-5 times higher than those of the other solutions.

These results are interesting considering that the molecular weights of PSS and Dex are more than three orders of magnitude larger that those of the other ions. These results agree with previous observations,[13-15] suggesting that the pores of the CNT paper are relatively large and able to accommodate ions with a wide range of sizes without significant detriment to electrode performance.

Electrolyte solvent.—Cyclic voltammograms showed that in a Li^+-containing nonaqueous electrolyte solution a large reduction response occurred which was not observed in other solutions. This behavior, attributed to the insertion of Li^+ in the interstitial spaces between nanotubes inside the bundles, was also observed previously for unannealed samples.[13-15] However, in that case, the response appeared at a potential 0.2 V more anodic, suggesting that intercalation in annealed samples is more difficult. Increased lithium intercalation has been associated with structural disorder and defects in CNT ropes.[9,17] The capacitance of annealed CNT paper in 0.1 M $LiClO_4$/acetonitrile was about 20% larger than in 0.1 M TBAHFP/acetonitrile and more than double that in aqueous 0.1 M $LiClO_4$,

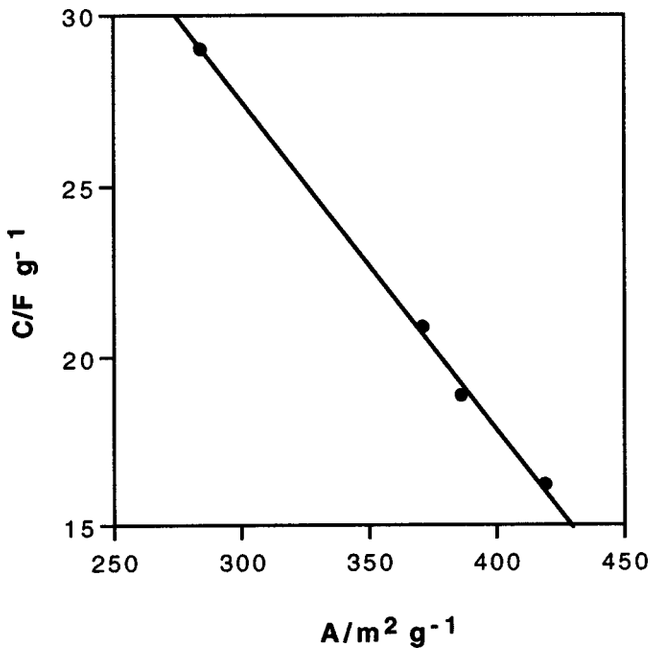

Figure 9. Capacitance (0.0 V, 1 M NaCl) as a function of BET surface area for annealed CNT papers.

suggesting that in an aprotic medium Li^+ interacts much more strongly with the CNT than any of the other ions investigated.

Effect of electrode thickness, surface area, and porosity

Thickness.—The capacitance and the charging time constant (R_1C) of CNT electrodes increase with increasing thickness of the CNT paper (Table I). This means that in thicker electrodes more charge can be stored or extracted, but at a lower rate. The trend observed can be mainly explained by the increasing surface area of the electrode that accompanies the growing thickness. At the thicknesses investigated, diffusion-controlled charging was not evident, perhaps again due to the relatively open structure of the porous material. However, the effect of increased thickness is clearly shown in the shift of the maximum in Bode phase-angle curves (not shown) towards lower frequencies, reflecting greater difficulty for the electrode to respond to the ac signal.

Surface area and porosity.—Sheets were prepared using varying amounts of CNT material to produce electrodes with increasing thickness, mass, and surface area. The capacitance of the samples in both 1 M NaCl and 0.1 M TBAHFP/acetonitrile was measured using EIS.

The correlation between the capacitance and surface area is shown in Fig. 9. On a mass basis, as the BET surface area increases, the electroactive surface area, of which the capacitance could be considered a measure, decreases. This is probably due to the solution having increasing difficulty reaching the inner areas of the CNT paper as the thickness increases. Even for solution-flooded pores, a decrease in the penetration of the time-dependent electrical signal can be expected as the pores become deeper with increasing thickness.

Assuming that the BET and electroactive surface areas are the same, the areal capacitance for the CNT papers evaluated is around 5 $\mu F/cm^2$, similar to the values reported for the basal plane of graphite measured under very well-controlled conditions.[20] However, if this assumption is not true, as Fig. 9 and porosity data presented below suggest, then the areal capacitance of the CNT paper must be higher than 5 $\mu F/cm^2$, perhaps as high as 10 $\mu F/cm^2$. This would not be unreasonable on two accounts. First, values higher than 5 $\mu F/cm^2$ have often been reported for the basal plane of graphite.[31] Second, for the CNT papers investigated, the surface structure is not as ordered and inert, and the purity not as high, as those encountered in the basal plane of graphite.

Pore size distribution was investigated for both annealed and unannealed CNT sheets prepared from aqueous dispersions. Pores are usually classified[32] into three groups according to their size: micropores (<2 nm), mesopores (2-5 nm) and macropores (>5 nm). The total surface area is also divided into two parts, the micropore area and the external area, which includes the area from mesopores and macropores.

A first important result is that the average pore size for both annealed and unannealed CNT sheets is around 9 nm (Table II). This relatively large value is consistent with our observation that the nature of the electrolyte does not markedly affect the basic response of the CNT electrodes, even when a wide range of ion sizes is involved. As established by many porosity studies of carbon materials,[32-34] pores larger than 0.5 nm are able to accommodate most common electrolyte ions. Although the CNT electrode contains a sizable fraction of micropore area that may not be accessible to the largest ions, a proportion of the micropores could still be penetrated by small ions and thus contribute to the double-layer capacitance at low charging rates, assuming the pores are wetted.

A significant consequence of the thermal treatment of samples is an increase in surface area of the order of 40%, originating mainly in the external surface area (Table II). The relative contribution of mesopores and macropores to the external surface area also changes, showing a shift towards a greater proportion of mesopore area, perhaps as a result of tighter packing of the nanotubes and bundles. The decrease in CNT electrode capacitance and the increase in surface area introduced by the annealing treatment suggest that the greater capacitance values associated with the unannealed samples are primarily due to the presence of electroactive impurities and surface functional groups. Clearly, the gain in capacitance due to increased surface area obtained upon annealing does not compensate the decrease arising from the loss of carbonaceous material and pseudocapacitance.

Conclusions

The electrochemical properties of porous CNTs electrodes in the form of sheets or papers have been further examined, particularly in terms of their frequency response. Thermal annealing has produced significant changes in a range of properties of the material, including increased hydrophobicity and elimination of electroactive surface functional groups and other impurities. As a result of these changes, the treated electrodes exhibit lower interfacial capacitance, absence of faradaic responses and associated pseudocapacitance, and a better frequency response.

The potential of zero charge and the capacitance dependence on frequency were similar to those described for the basal plane of graphite, with some differences due in part to the inhomogeneous nature of the CNT paper surface. This behavior, as well as the varia-

Table II. Porosimetry data for CNT samples.

Sample	Total area (m^2/g)	Micropore area (m^2/g)	External area (m^2/g)	Mesopore area (%)	Macropore area (%)	Average pore size (nm)
Unannealed	173.2	107.2	66.1	10	87	8.7
Annealed	247.2	114.9	132.3	25	72	8.8

tion of electrode resistance with applied potential, has been attributed to the semiconducting nature of certain types of CNTs.

The basic electrochemical behavior of the CNT paper electrodes is not markedly affected by relatively large differences in the nature of the electrolyte. Analysis of pore size distribution indicates that the CNT sheets exhibit an average pore size of 9 nm, consistent with the ability to charge at relatively fast rates and the possibility to operate in electrolytes containing bulky ions without significant loss of performance.

Increase in both CNT sheet thickness and surface area induce a slower electrode response as the electrolyte and the electrical signal find increasing difficulty in penetrating the pores of the electrode matrix.

Acknowledgments

This work was partially supported by U.S. Defense Advanced Research Project Agency grant N00173-99-2000. G. G. Wallace acknowledges the continued support of the Australian Research Council. The porosimetry analysis performed by Particle and Surface Sciences Pty. Ltd., Australia, is gratefully acknowledged.

References

1. S. Subramoney, *Adv. Mater. (Weinheim, Ger.)*, **10**, 1157 (1998).
2. P. M. Ajayan, *Chem. Rev. (Washington, D.C.)*, **99**, 1787 (1999).
3. H. Hu, T. W. Odom, and C. M. Lieber, *Acc. Chem. Res.*, **32**, 435 (1999).
4. *Science and Applications of Nanotubes*, D. Tomanek and R. J. Enbody, Editors, Kluwer/Plenum, New York (2000).
5. *Carbon Nanotubes: Synthesis, Structure, Properties and Applications*, M. S. Dresselhaus, G. Dresselhaus, and P. Avouris, Editors, Springer-Verlag, Heidelberg (2001).
6. K. H. An, W. S. Kim, Y. S. Park, J. M. Moon, D. J. Bae, S. C. Lim, Y. S. Lee, and Y. H. Lee, *Adv. Funct. Mater.*, **11**, 387 (2001).
7. C. Niu, E. K. Sichel, R. Hoch, D. Moy, and H. Tennent, *Appl. Phys. Lett.*, **70**, 1480 (1997).
8. A. S. Claye, J. E. Fisher, C. B. Huffman, A. G. Rinzler, and R. E. Smalley, *J. Electrochem. Soc.*, **147**, 2845 (2000).
9. G. T. Wu, C. S. Wang, X. B. Zhang, H. S. Yang, Z. F. Qi, P. M. He, and W. Z. Li, *J. Electrochem. Soc.*, **146**, 1696 (1999).
10. R. H. Baughman, C. Cui, A. A. Zakhidov, Z. Iqbal, J. N. Barisci, G. M. Spinks, G. G. Wallace, A. Mazzoldi, D. De Rossi, A. Rinzler, O. Jaschinski, S. Roth, and M. Kertesz, *Science*, **284**, 1340 (1999).
11. G. M. Spinks, G. G. Wallace, R. H. Baughman, and Liming Dai, in *Electroactive Polymer Actuators as Artificial Muscles*, Y. Bar-Cohen, Editor, p. 223, SPIE, Washington, DC (2001).
12. Unpublished results.
13. J. N. Barisci, G. G. Wallace, and R. H. Baughman, *J. Electroanal. Chem.*, **488**, 92 (2000).
14. J. N. Barisci, G. G. Wallace, and R. H. Baughman, *Electrochim. Acta*, **46**, 509 (2000).
15. J. N. Barisci, G. G. Wallace, and R. H. Baughman, *J. Electrochem. Soc.*, **147**, 4580 (2000).
16. A. G. Rinzler, J. Liu, H. Dai, P. Nikolaev, C. B. Huffman, F. J. Rodriguesmacias, P. J. Boul, A. H. Lu, D. Heymann, D. T. Colbert, R. S. Lee, J. E. Fisher, A. M. Rao, P. C. Eklund, and R. E. Smalley, *Appl. Phys. A: Solids Surf.*, **29**, 67 (1988).
17. E. Frackowiak, S. Gautier, H. Gaucher, S. Bonnamy, and F. Beguin, *Carbon*, **37**, 61 (1999).
18. H. Keiser, K. D. Beccu, and M. A. Gutjahr, *Electrochim. Acta*, **21**, 539 (1976).
19. H. K. Song, H. Y. Hwang, K. H. Lee, and L. H. Dao, *Electrochim. Acta*, **45**, 2241 (2000).
20. J. P. Randin and E. Yeager, *J. Electroanal. Chem. Interfacial Electrochem.*, **36**, 257 (1972).
21. Y. Orem and A. Soffer, *J. Electroanal. Chem. Interfacial Electrochem.*, **206**, 101 (1986).
22. D. Golub, Y. Orem, and A. Soffer, *Carbon*, **25**, 109 (1987).
23. H. Gerisher, R. McIntyre, D. Scherson, and W. Storck, *J. Phys. Chem.*, **91**, 1930 (1987).
24. B. Kastening, M. Hahn, and J. Kremeskötter, *J. Electroanal. Chem.*, **374**, 159 (1994).
25. B. Kastening, M. Hann, B. Rabanus, M. Heins, and U. zum Felde, *Electrochim. Acta*, **42**, 2789 (1997).
26. M. G. Sullivan, R. Kötz, and O. Haas, *J. Electrochem. Soc.*, **147**, 308 (2000).
27. R. Jacquemin, S. Kazaoui, D. Yu, A. Hassanien, N. Minami, H. Kataura, and Y. Achiba, *Synth. Met.*, **115**, 283 (2000).
28. P. Blanc, A. Larbot, J. Palmeri, M. Lopez, and L. Cot, *J. Membr. Sci.*, **149**, 151 (1998).
29. B. E. Conway, *Electrochemical Supercapacitors*, Chap. 17, Kluwer/Plenum, New York (1999).
30. Y. Oren and A. Soffer, *J. Electroanal. Chem. Interfacial Electrochem.*, **186**, 63 (1985).
31. K. Kinoshita, *Carbon: Electrochemical and Physical Properties*, p. 294, Wiley, New York (1998).
32. B. E. Conway, *Electrochemical Supercapacitors*, Chap. 14, Kluwer/Plenum, New York (1999).
33. A. Soffer, D. Golub, and Y. Oren, *J. Electroanal. Chem. Interfacial Electrochem.*, **260**, 383 (1989).
34. D. Qu and H. Shi, *J. Power Sources*, **74**, 99 (1998).